

Non-Classical Conductor Losses due to Copper Foil Roughness and Treatment

Gary Brist and Stephen Hall
Intel Corporation
Hillsboro, OR

Sidney Clouser
Gould Electronics
Eastlake, OH

Tao Liang
Intel Corporation
Hudson, MA

Abstract

In high speed digital interconnects; signal attenuation is a result of both dielectric losses and conductor losses. Previous works have showed in detail, the characterization and modeling efforts regarding the impact of dielectric loss in PCBs and the differences between various dielectric materials. Most high speed characterization modeling efforts have not encompassed the variations in conductor losses due to variations in copper foil roughness or treatments of copper foil for adhesion. Several recent publications have reported frequency dependent copper losses that do not follow the classical square root relationship. This paper presents the results for a set of high frequency loss characterizations across various copper foils and the impact of the copper roughness on the relationship between conductor loss and frequency. Also discussed in this paper are the implications in high frequency modeling resulting from non-classical conductor losses and the requirements to ensure causality in simulation results.

Introduction

Copper foil is roughened to promote adhesion of the dielectric resin to the conductor in printed circuit boards. Adhesion at the interface between conductor and insulator must be very robust due to conditions during manufacturing, assembly, and standard usage to which a printed circuit board is subjected. This interface is exposed to corrosive chemicals during processing and to high temperature, high humidity, cold, shock, vibration, and shear stresses during use. Technologies that optimize surface and resin chemistries, as well as surface area, are utilized by foil manufacturers and laminators to promote and retain adhesion¹.

The copper foil roughness and adhesion are related. Adhesion is quantified by measuring the 90-degree peel strength per IPC-TM 650 2.4.8C. Factors which contribute to mechanical adhesion, according to the elastic theory, are the thickness of the deformed resin y_0 , the tensile strength of the resin σ_N , the foil thickness δ , and the ratio of the copper modulus, E to the resin modulus, Y . Roughness enters into this theory through the adhesive interlayer thickness, y_0 . As shown in Figure 1, the adhesive interlayer thickness is correlated to the treatment height. Higher roughness increases the interlayer thickness, the surface area, and the chemical contributions to peel strength. Though roughness contributes positively to peel, it has a negative impact on signal integrity.

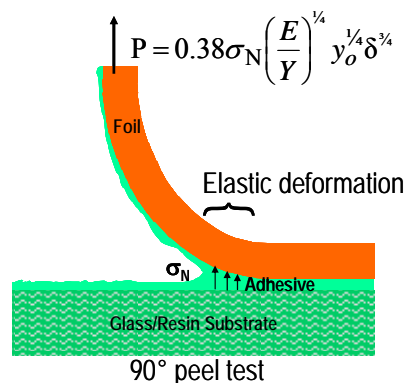


Figure 1 - Copper Foil Adhesion

The impact of copper foil roughness on signal integrity effects modeling, design, and, ultimately, the material selection for printed circuit boards. Most designers are familiar with the increase in transmission line resistance due to skin effect as frequencies increase. The conductor resistance increases from a redistribution of the currents to the outer regions of a conductor cross-section as frequency is increased. In smooth conductors, the relationship of the current density and frequency is known as the skin depth. In a smooth conductor, 67% of the current flowing in the conductor resides in the region that is one skin depth from the surface. This skin depth reduces inversely with the square root of frequency and translates into a resistance that increases with the square root of frequency. At low frequencies, the conductor loss associated with a printed circuit board traces behave much the same. As the predominate signaling frequencies in today’s electronic designs increase, the skin depth approaches the value of the copper foil roughness. See Figure 2. As a result, the measured conductor loss in printed circuit board traces no longer conforms to the classical skin resistance models.

In order to experimentally quantify the copper foil roughness relationship with conductor loss, a set of test boards were built using different 18µm copper foil grades, each with different foil roughness. To minimize manufacturing differences between test samples, all foil samples were laminated to the same dielectric material, of the same material lot, and processed through lamination, drill, plating and etch together as one production lot. Throughout the process, physical and electrical measurements were taken to note any differences between the foil grades that would impact the electrical performance of the test vehicles or alter modeling efforts. High frequency S-parameter measurements were obtained for each copper foil type and comparisons made. The measured results were then used to explore modeling approaches and determine which modeling methodology captured the impact of copper foil roughness without violating model causality.

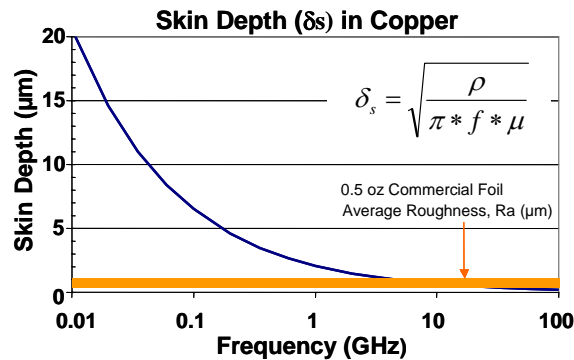


Figure 2 - Skin Depth vs. Frequency

Copper Foils

The 18 µm thick copper foils in this study ranged from very smooth to rough. See Table 1. These foils included one rolled copper foil and five electrodeposited copper foils. Figure 3 and Figure 4 show the differences in roughness as seen by SEM and by cross-section respectively. The smoothest surface was the rolled copper foil with no surface treatment for roughening. Untreated rolled copper typically has unacceptably low adhesion for commercial use, but, as a treated foil is widely used in flexible circuits.

Table 1 - Copper Foil Types and Surface Roughness Used In High Frequency Tests

Material	Roughness (µm)				Resistivity	Copper Surface and Bond Treatment Roughening
	Profilometer		WYKO		after lamination	
	R _a	R _{tm}	R _a	R _t	µOhm*cm	
JTCSHP	0.75	6.3	1.31	10.9	1.88	Matte side high profile, heavy nodule
RTCHP	0.60	5.1	0.69	7.9	1.85	Shiny side, heavy nodule
AMFN	0.48	3.8	Black		1.90	Matte side very low profile, fine nodule
RTC	0.45	3.6	0.62	7.9	1.82	Shiny side, medium nodule
TCR	0.50	4.5	0.65	6.6	1.76	Matte side, no nodule, 100 Å NiCr layer
Rolled	0.39	3.2	0.25	4.5	1.71	Shiny side, no nodule

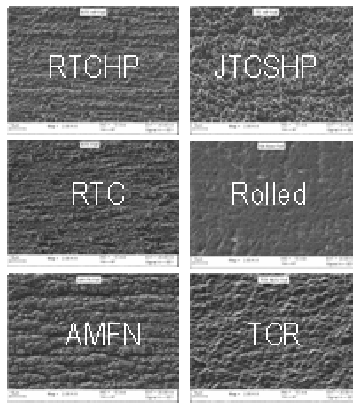


Figure 3 - SEM of Copper Foil Grades

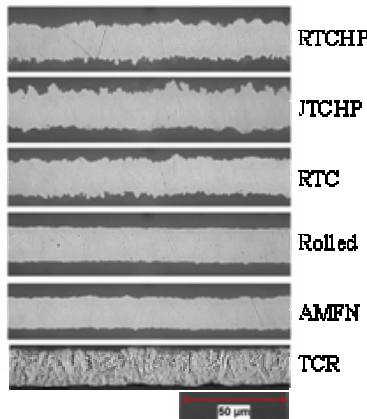


Figure 4 - Cross Section of Copper Foil Grades

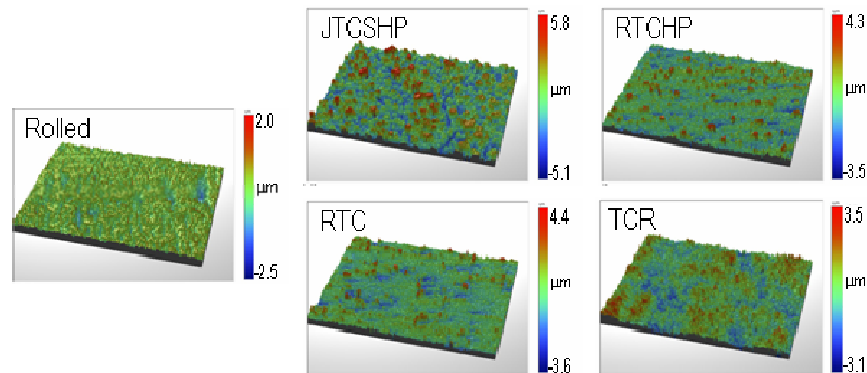


Figure 5 - Optical Profile of Copper Foils

The AMFN, RTCHP, RTC, JTCSHP, and TCR foil tested were electrodeposited foils. Roughness on these foils is controlled by applying levels of nodular copper treatment to either the shiny or the matte side of electrodeposited copper foil. The very low profile AMFN, and the foils with nodular treatment on the shiny side, RTCHP and RTC, are relatively smooth and typically used to construct innerlayers. Foil with treatment on the matte side, JTCSHP, is rough by comparison and usually used on outerlayers. TCR foil has a matte surface with a NiCr layer, without nodules, and is used to form embedded resistors.

Copper foil surfaces were critically defined for this study. The surface metrology was measured by stylus profilometer using a Taylor-Hobson Surtronic 3 (IPC method 2.2.17A), by non-contact optical profiling using a WYKO NT 1100, by scanning electron microscopy, and by cross-section photomicrographs. The measurements are summarized in Table 1, and surface morphologies shown in the Figure 3, Figure 4, and Figure 5.

Comparison of the roughness of commercial copper foil and the foils in this study is shown in Figure 6. The commercial foil roughness distributions are from the database maintained by the manufacturing facilities of Nikko-Materials/Gould. The roughness and treatment of each foil type is customized to meet local customer requirements of roughness and adhesion to a

specific resin system. The treated side roughness of each lot of electrodeposited copper foil is measured as $R_{tm} = R_z$ (DIN) using a stylus profilometer per IPC method 2.2.17A. A lot size ranges from 80 to 25,000 m^2 . The roughness distribution of all lots of each type of 0.5 oz/ft² copper foil is plotted in the figure. The surface roughness of foils in this study spanned the range of the commercial copper foils.

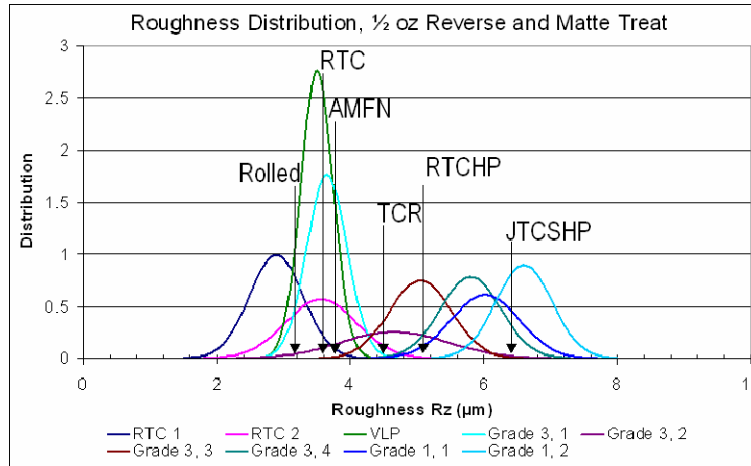


Figure 6 - Comparison of 0.5 oz Foils Produced Globally and This Study

Test Vehicle

The set of test boards were fabricated using a portion of Intel’s material characterization test board design³. To improve the ratio of conductor loss to dielectric loss, Nelco N4000-13 was selected. The six copper foils used in the testing were laminated to 5mil Nelco N4000-13 prepreg at Gould.

The individual di-clad laminates were then drilled, plated and patterned. No soldermask was applied to minimize dielectric losses. The boards were then coated with Immersion Silver. The Immersion Silver surface finish was selected to minimize the impact to the high frequency measurements¹¹. The pattern on each test boards contained 5mil and 15mil wide traces in 1inch, 3inch, and 5inch line segments.

The probe pattern for each of the test traces was designed to be tested with 250 μ m pitch GSG (Ground-Signal-Ground) probes. See Figure 7 and Figure 8. The traces of like width and length were placed on 140mils centers to reduce the coupling to adjacent traces during measurement. See Figure 9. These groupings were then placed multiple times in multiple rotations across each panel.

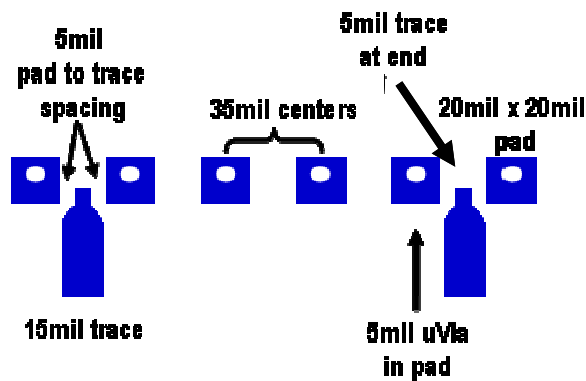


Figure 7 - GSG Probe Launch for 5mil Traces

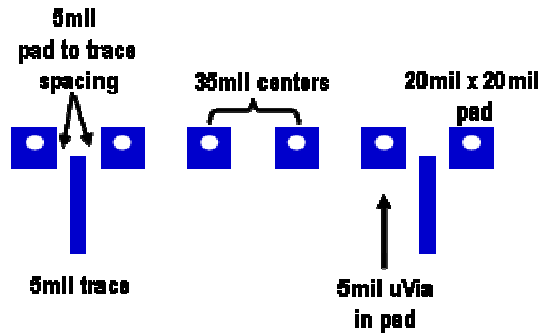


Figure 8 - GSG Probe Launch for 15mil Traces

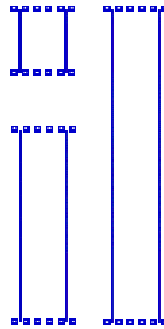


Figure 9 - Trace Groupings As Measured

Measurement Results

The physical trace data from the different copper types is summarized in Table 2. The dielectric and conductor physical parameters for each of the structures across the copper types were essentially identical, within measurement error, except the conductor width of the rolled annealed copper structures. The lack of nodular treatment on the rolled annealed copper creates a faster etching of the foil and resulted in a 0.4 - 0.5mil over etching of the structures. This resulted in a slightly higher impedance and higher conductor loss as measured and required a corresponding change in the simulation models for rolled annealed copper structure.

For each copper type, 6 measurements were taken for each of the 5mil and 15mil line widths for both 5inch and 3inch trace lengths. In total, 24 measurements were taken for each copper type. Measurements of each trace were obtained using an Agilent Vector Network Analyzer (VNA) to obtain S-parameters of each structure. For each S-parameter set, the transmission line loss was calculated across the frequency sweep by using the identity of loss, denoted by α , as being the real part of gamma, γ , as defined in equation 1a-1g. These set of identities allowed for accurate computation of the transmission line loss across transmission lines of different impedance from the calibration standard. Figure 10 shows the measured impedance of the traces as a function of copper type. The 5mil traces on the electrodeposited copper foil had impedances between 64 and 69 ohms with the rolled copper foil having the highest impedance resulting from the narrower line widths. The 15mil traces followed the same trend with the electrodeposited copper foil having a typical impedance of 34-38ohms and the rolled copper foil having a slightly higher impedance.

Table 2 - Physical Measurements of Samples

Copper type	Dielectric thickness (mils)	5mil trace width (mils)	15mil trace width (mil)	Trace thickness (mil)
JTCHP	4.7	4.3	14.3	2.1
RTCHP	4.8	4.1	14.1	2.1
AMFN	4.8	4.3	14.3	2.1
RTC	4.9	4.2	14.2	2.1
Rolled	4.9	3.6	13.6	2.2
TCR	4.8	4.2	14.2	2.1

$$1a) \Gamma_{Short} = S_{11} - \frac{S_{12} S_{21}}{1 + S_{22}} \quad 1b) \Gamma_{Open} = S_{11} + \frac{S_{12} S_{21}}{1 - S_{22}}$$

$$1c) Z_{inShort} = Z_0 \frac{1 + \Gamma_{Short}}{1 - \Gamma_{Short}} \quad 1d) Z_{inOpen} = Z_0 \frac{1 + \Gamma_{Open}}{1 - \Gamma_{Open}}$$

$$1e) \gamma = \text{arcTanh} \left(\sqrt{\frac{Z_{inShort}}{Z_{inOpen}}} \right) = \sqrt{(R + j\omega L)(G + j\omega C)}$$

$$1f) \alpha_{measured} \equiv \Re\{\gamma\} \text{ in Nepers / length}$$

$$1g) \text{ Nepers / meter} = 8.686 \text{ dB / inch}$$

Equation 1 - Transmission Line Equations

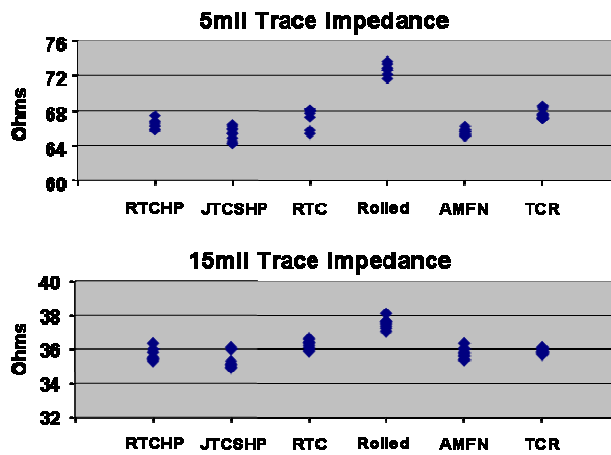


Figure 10 - Impedance by Copper Type

Electrical Loss Measurements

The summary of the measured transmission line loss across the different copper types is shown in Figure 11. The measured loss for the 1inch, 3inch, and 5inch traces had the same dB/inch loss across the frequency range. The differences between multiple measurements of the same copper type were tightly grouped and did not show much variation.

The measured results showed that the rougher copper foils resulted in higher transmission line losses. Rolled copper foil had the lowest overall loss even with a narrower trace width. Simulation showed that the transmission lines on the rolled copper foil would have had roughly a 0.055dB/inch lower loss at 20GHz if the conductor width been similar the other foils. The higher losses in the roughest copper foils (JTCSHP and RTCHP) were significant at frequencies greater than 2.0GHz. Additionally, the losses for JTCSHP copper were higher than rolled by 0.3-0.40dB/inch at 10GHz.

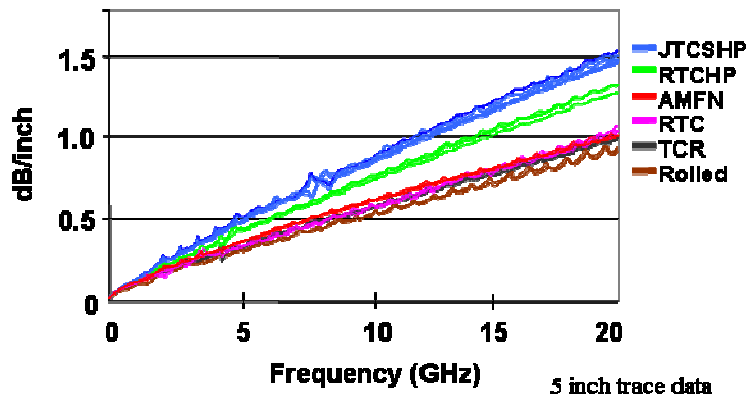


Figure 11 - Total Line Loss by Copper Type

Modeling Conductor Loss with Roughness

Initial models were developed in HFSS using the measured physical dimensions of the various transmission lines across the different copper foils assuming no surface roughness. Each model was developed based on the measured cross section geometries of each transmission line, the measured conductivity of the particular copper foil type, and the dielectric constant and dielectric loss properties of N4000-13 material. The N4000-13 material properties were obtained from split post resonator measurements at 1GHz. As expected, the initial models did not match the measured results because there was no accounting for the impact of surface roughness. Figure 12 shows the comparison between the measured loss for RTCHP and rolled copper compared to HFSS models that do not account for surface roughness. The rolled copper, which is the smoothest sample tested, correlated well to measurements because the roughness has minimal effect, however, the RTCHP structure, which exhibits significant roughness, deviated significantly from the measurement above 2 GHz.

In analyzing the measured results, several techniques were found that could be incorporated to generate a loss model that matched the measured results across frequency. The first technique involved considering how the different copper types behaved at low frequencies. Figure 13 shows the curve fitting of the measured loss curves for each copper type. By adjusting the classical skin effect conductor losses to a higher power than the square root of frequency a good match was obtained. The issue with this method was that the modified power parameter required to ensure a good model fit varied by copper roughness and also varied by line width.

The second technique looked at how the different copper types varied at higher frequencies. At frequencies greater than 1GHz, the difference between the copper types were almost linear with respect to frequency and it was found that the higher loss due to the copper foil roughness could be modeled as an effective increase in the dielectric loss tangent (tand) of the dielectric material. This method has been used in the past by designers, as the material tand is a property easily changed in modeling environments. Designers have partially justified this method based on the uncertainty and variation in reported loss tangents for a given material due to differing metrologies. Although this method works well for modeling transmission line losses; it requires different values based on line width geometries for a given copper foil roughness. See Figure 14.

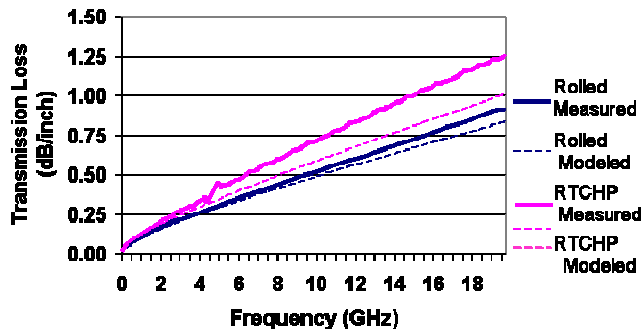


Figure 12 - Measured vs. Classic Models

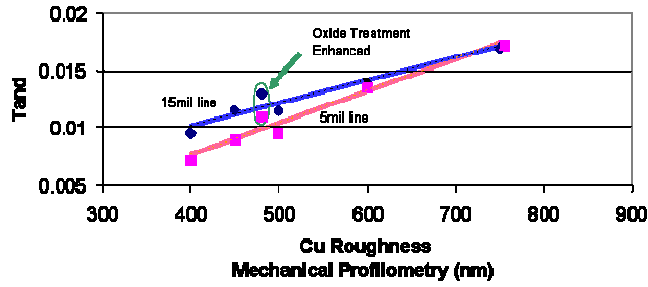


Figure 13 - Low Frequency by Copper Foil Type

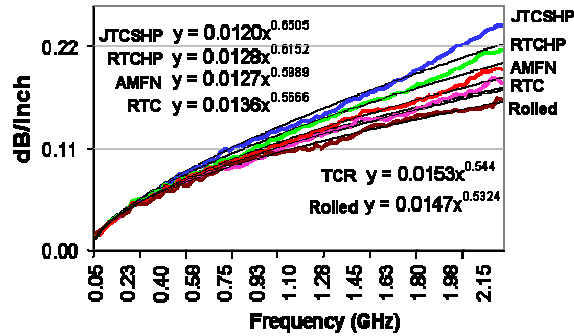


Figure 14 - Effective Tand vs. Cu Roughness

With both of these techniques, the factor required to achieve a match between modeled and measured losses was not solely based on the copper foil roughness; but, also line width. This makes it difficult to determine a usable factor that can be easily incorporated across multiple design teams Hammerstad and Jensen proposed an empirical formula that can be used to effectively model the frequency dependent loss, through an additional loss factor to the classical conductor attenuation coefficient for a smooth surface based explicitly on the copper foil roughness.⁴

$$\alpha_c' = \alpha_c * K_{sr} \quad \text{Eq. 2}$$

In equation 2, α_c' is the attenuation coefficient due to conductor loss with surface roughness effect included, and α_c is the attenuation coefficient with smooth conductor. K_{sr} is calculated through the following empirical formula derived from microstrip line measurements:

$$K_{sr} = 1 + \frac{2}{\pi} \arctan[1.4(\frac{\Delta}{\delta})^2] \quad \text{Eq. 3}$$

In equation 3, Δ is the surface roughness RMS value and δ is the skin depth. In Figure 15, K_{sr} is plotted with different RMS values as a function of frequency. Notice that K_{sr} equals 1 at DC and asymptotically approaches 2 at high frequencies.

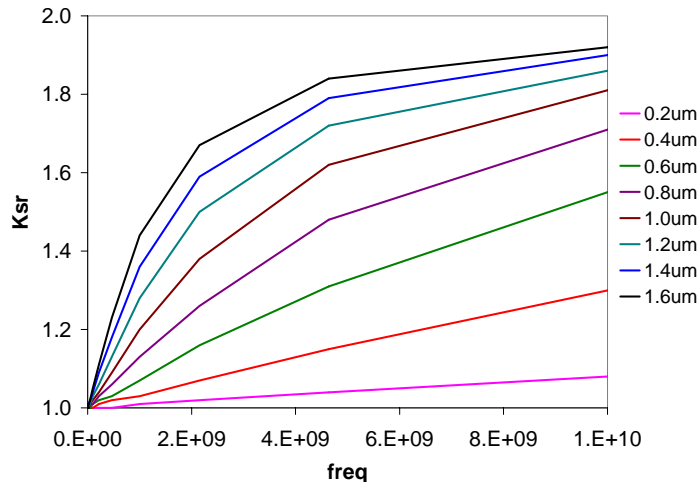


Figure 15 - Loss Factor K_{sr} due to Surface Roughness Effect

Using the approach proposed by Hammerstad and Jensen, a very good correlation was obtained between the modeled and the measured transmission line losses across the copper types. This technique was found to be superior to the effective tand approach and to the modified skin effect approach because it was based solely on the physical measured copper foil roughness.

Causality and Conductor Loss Modeling

In order to correctly model the propagation of a signal on a transmission line, it is necessary that the complex impedance function be analytic⁸. Consequently, a change in the impedance must correspond to a specific change in the loss. These relationships govern the amount of energy that is propagated down the transmission line versus the amount of energy that is dissipated through the conductor and dielectric losses. Assumptions that violate this principle effectively cause a portion of the signal to be propagated when it should have been attenuated, or visa-versa. The classical assumption of frequency invariant transmission line parameters induces non-causal behavior by propagating energy that should have been attenuated, and thus violates conservation energy principles.

In order for a model to produce a real, causal response in the time domain, the transfer function of the transmission line must satisfy the following constraints:

Equation 4 ensures that the impulse response of the system is real while equation 5 ensures that it is causal^{10, 11}. Equation 4-5 necessitates that the real and imaginary parts of the frequency response obey the Hilbert Transform relationships, which enforce interdependency between the dielectric constant and the loss tangent, as well as the inductance and skin losses.

A draw back of the techniques listed so far for modeling the loss due to the copper foil roughness is that they violate equation 5 and result in non-causal time domain responses. It can be shown that modifying the effective tand of the material without simultaneously modifying the material dielectric constant violates the requirements of equation 5. Similarly, adjusting the skin effect conductor losses to a higher power than the square root of frequency also violates equation 4 and 5.

The Hammerstad and Jensen approach can be forced to meet the causality requirements by a simple adjustment which makes the loss factor an even function with respect to frequency as shown in Equation 6.

$$H(-\omega) = H^*(\omega) \quad \text{Eq. 4}$$

$$h(t) = 0 \quad \text{for } t < 0 \quad \text{Eq. 5}$$

$$K_{sr} = 1 + \text{sgn}(\omega) \frac{2}{\pi} \arctan[1.4 \left(\frac{\Delta}{\delta}\right)^2] \quad \text{Eq. 6}$$

To accurately predict the losses of a microstrip transmission line, it is necessary to account for the surface roughness using equation 6 and the frequency dependence of tand. Furthermore, the correct variation of tand and its interdependence to the dielectric constant with respect to frequency must be maintained for real, causal time domain responses. The interdependency between the dielectric constant and tand can either be measured with split post resonator methods or calculated by the method present in reference.¹⁶ Figure 16, Figure 17, and Figure 18 show the measured loss and the results of the different modeling techniques. The classic model did not compensate for surface roughness and also assumed a constant tand across the frequency range. The tand technique and, the copper power technique correlated to the measurement well, however, did show larger errors than the causal model below 2GHz as seen in Figure 18. The casual model provided the best results across the entire frequency range. The model using the roughness adjustment and assuming a constant tand was also plotted showing increased error with frequency, which bolsters the necessity of incorporating both the copper foil roughness and a frequency dependent tand that varies with frequency for good model accuracy.

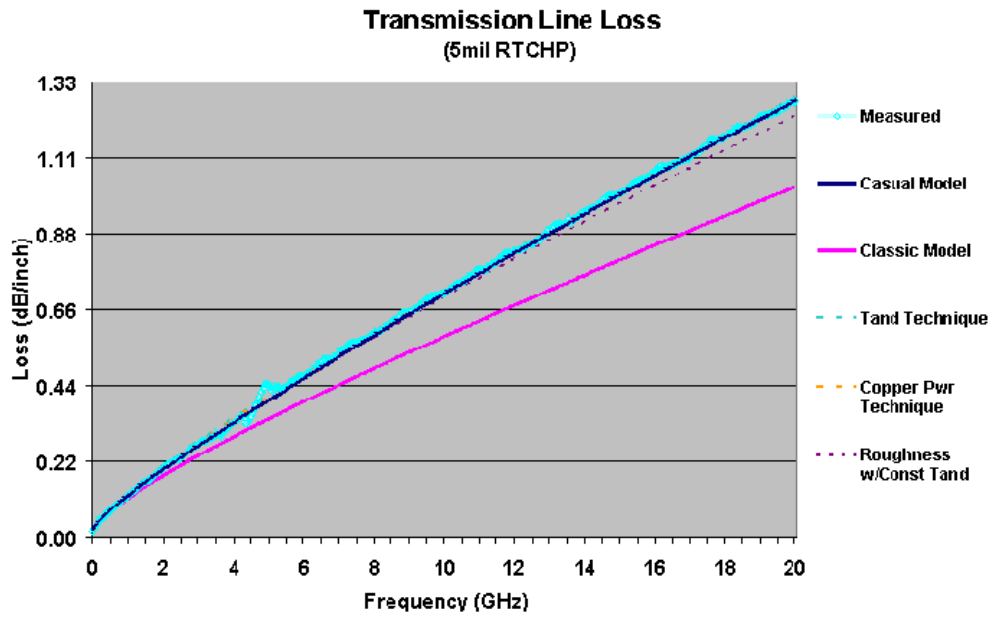


Figure 16 - Modeled Transmission Line Loss

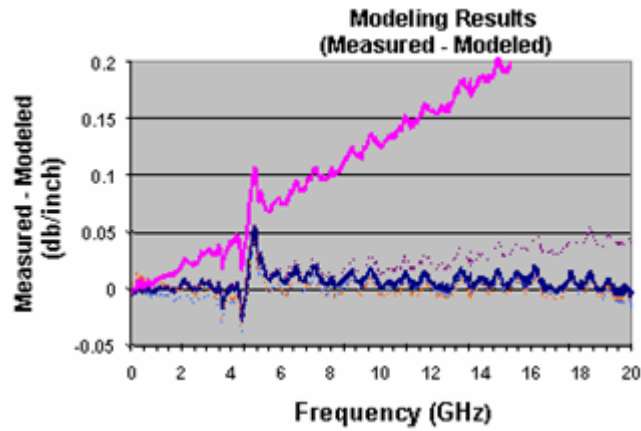


Figure 17 - Modeling Errors

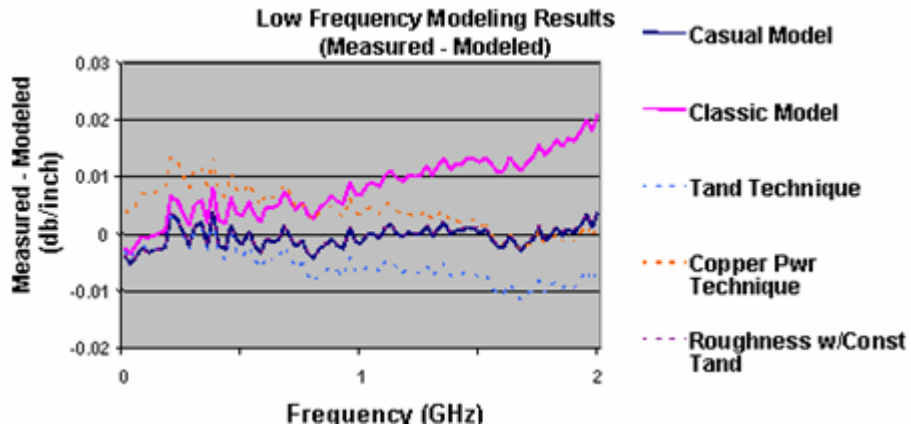


Figure 18 - Modeling Errors at Low Frequency

Summary

The work shown in this paper demonstrated that the copper foil roughness significantly increases the measured loss of a microstrip transmission line. Furthermore, several methods for integrating the copper roughness effects into transmission line models were discussed. It was shown that the mechanical roughness measurements of the foil directly correlated to the added transmission line loss and from a mechanical adhesion perspective there is a trade off between smoothness of copper foil and electrical performance. It was noted that different copper foil type not only exhibited different surface roughness and electrical loss; but also exhibited different process variations in final line widths, overall thickness and bulk conductivity.

There are multiple methods for incorporating the additional transmission line loss due to copper roughness into electrical models. This paper discussed three methodologies that have been published and the limitations of each. Two of the methods, adjusting the skin effect's square root of frequency relationship or adjusting the material tand could be used, however, both were found impractical because the adjustments were dependent on both the copper roughness and actual line width. The most practical method was based on the modified Hammerstad and Jensen equation to scale the skin effect losses to account for surface roughness. This method was preferred because it is based on physically measurable attributes and has been shown to preserve causal time domain responses.

Most importantly, it was found that to obtain an accurate model over a wide frequency range the copper roughness had to be included as well as the proper interaction between dielectric constant, dielectric loss, and frequency.

References

1. L. Valette, R. Wiechmann, "High-performance substrate from new epoxy resin and enhanced copper foil", *Circuit World*, 30(4), 20 (2004).
2. J. McCall, D. Shykind; "Non-Ideal Frequency Dependant Loss in Realistic PCB Transmission Lines," IEEE, (April 2002)
3. G. Brist, J. McCall; "Spatial Impact of PCB Fabrication and Materials on Single-Ended and Differential Impedance Transmission Lines," PCB West/HDI Expo 2003, (March 2003)
4. Hammerstad and Jensen, "Accurate Models for Microstrip Computer-Aided Design", IEEE MTT-S Digest, pp407-409, May 1980
5. G. Brist, G. Long, D. Sato; "Optimized System Design Through Industry Benchmarking of Fabrication Tolerances and Material Properties," Fall IPC Mtg, (November 2003)
6. K. Dietz; "Fine Lines in High Yield (Part XCVIII): Advances in Reinforcement Structures "; *Circuitree*; Nov 2003.
7. G. Brist, B. Horine, G. Long; "High Speed Interconnects: The Impact of Spatial Electrical Properties of PCB due to Woven Glass Reinforcement Patterns," IPC Expo 2004, (February 2004).
8. Ramo, S, et. al., *Fields and Waves in Communication Electronics, 2nd Edition*, John Wiley & Sons, 1965.
9. R. Matick, *Transmission Lines for Digital and Communication Networks*, IEEE Press, 1995
10. Arabi, T, et. al., "On the Modeling of Conductor and Substrate Losses in Multi-Conductor Transmission Line Systems," IEEE Transactions on Microwave Theory and Techniques, Vol. 39, No. 7, July 1991.
11. A. Djordjevic, "Wideband Frequency Domain Characterization of FR4 and Time Domain Causality," IEEE Transactions on Electromagnetic Compatibility, Vol. 43, No. 4 November 2001.
12. H. Heck, B. Horine, J. McCall, T. Liang, G. Brist; "The PCB Technology Evolution for 10 Gb/s & Beyond," Intel Technology Symposium, September 17-18, 2003.
13. H. Heck, B. Horine, S. Hall, K. Mallory, T. Wig; "Impact of FR4 Dielectric Non-Uniformity on the Performance of Multi-Gb/s Differential Signals,"; IEEE 12th Topical Meeting on Electrical Performance of Electronic Packaging, October 27-29, 2003, Princeton, NJ pp. 243-246.
14. S. Hall, G. Hall, J. McCall, *High-Speed Digital System Design – A Handbook of Interconnect Theory and Design Practices*, Wiley & Sons, 2000
15. D. Cullen, B. Klein, G. Moderhock, L. Gatewood; "Effect of Surface Finish on High-Frequency Signal Loss Using Various Substrate Materials." IPC EXPO, (March 2001)
16. S. Hall, et. al., "Modeling Requirements for Transmission Lines in Multi-Gigabit Systems," IEEE Electrical Performance of Electronic Packaging Symposium, October 25-27, 2004, pp, 67-70